Interaction Notes

Note 551

October 1998

The test-wiring method

Jean-Philippe Parmantier
ONERA, 8 rue des Vertugadins, 92190 Meudon, FRANCE

Abstract

This paper describes a technique allowing one to determine the voltage generator distribution to apply on the cable-network model of a wiring excited by an external field. This method is particularly well suited for wiring installed inside real structures for which the numerical determination of the incident field along the wiring paths is often illusory. The method deals with replacing the complex wiring under study by a so-called "*test-wiring*" running at the same location. The test-wiring has to be chosen the most simple as possible if one wants to be able to model it with a cable-network model, less constraining than a 3D code. Generally, the test-wiring is made of one-wire cables connected to each other. This modeling provides the so-called "*Green's function matrix*" of the test-wiring, relating distributed currents along the wires and the distribution of voltage generators giving birth to those currents.

Therefore, measuring a set of currents on the test-wiring inside the real structure excited with an EM field allows one to come back to the equivalent generators driving the EM coupling on the real wiring problem. Indeed, those generators are closely related to the incident tangential fields along the wiring. Consequently, they can be applied in any cable model configuration, provided that the modeled cables run in the same place as the test-wire. The test-wiring acts like a sensor of tangential electric field.

In this paper, the method relies on the realistic physical approximation that the equivalent generator is always equal to the incident tangential electric field. Numerical and experimental validation examples are presented to demonstrate the pertinence of the method in an industrial context. In addition, it is shown how such a kind of inverse problem resolution could provide in the future an efficient technique to detect localized interference sources onto a sensitive wiring.

Key-words :

Electromagnetic Topology ; Linear Systems ; Current injectors and current probes ; Transmission Lines ; Electromagnetic Compatibility ; Electromagnetic Coupling

Acknowledgments :

The author wants to thank the Prospective Bureau of DGA and AFOSR for having made possible the foreign assignment at the Kirtland Air Force Base (Albuquerque), during which this paper has been written.

Contents :

1. Introduction

In the field of Electromagnetic Coupling on wiring systems, the knowledge of the exciting source is at least as important as the modeling of the cable network itself. For Electromagnetic (EM) illuminations, the problem is made even more complex because of the distribution of sources all along the wiring.

Since 1991, recent progresses achieved in EM Topology [1] have demonstrated that the multiconductor network transmission-line formalism was ideally suited to analyze coupling on cable systems, provided that one was able to feed the topological network with elementary models of tubes, junctions and, especially, sources [2]. Recent studies carried out with the EM Topology based CRIPTE computer code [3] have demonstrated the capability to calculate equivalent sources along a cable network thanks to a three-dimension (3D) computer code ([4], [5]). This particular approach is mainly devoted to carry out predictive calculations on systems that do not already exist at the time of the analysis. Whereas certainly the most achieved of nowadays numerical strategy, this approach still presents two main drawbacks :

- at the present time, even if the wiring system is not to me meshed in a 3D model, it is not always possible to account for the high degree of complexity of the scattering structures in 3D numerical codes,
- 3D calculations are time and memory consuming and require high performance calculators that some laboratories cannot always afford.

These are the reasons why, in the conception phase of industrial programs, experiments on mock-ups or real systems are always carried out. In those phases however, numerical codes can still have an interesting role to play because of the help they can provide for the analysis of the measured data. For example, in the past ten years this has been emphasized in all the experiments that ONERA has performed with its collaborators in EM Topology problems ([4], [5], [6], [7]). Once validated, the numerical tools allow one to perform physical interpretations impossible to achieve with experimental data only.

In order to determine sources distributed all along a wiring path, the objective of this paper is to present a technique involving both measurements and numerical simulations performed with a cable-network code. The basic concept deals with the determination of the induced distributed currents coming from the real illumination on a so-called *"test-wiring"* running at the same location as the real cable bundle under study. Then, the resolution of an inverse problem on the test-wiring, based on reasonable physical approximations, provides the equivalent sources to apply on the real cable harness.

For this purpose, the cable-network formalism applied for the treatment of EM coupling on cable systems presents the main advantage of allowing the introduction of hybrid data to feed the models. For instance, in the CRIPTE code developed at ONERA, data for tubes, junctions and sources may come from analytical formulas, from other numerical calculations (3D codes, electrical circuit codes) or from measurements.

This paper is a concatenation of different results obtained between 1993 and 1998 and describes how our vision of the methodology has developed during those years. The first section of this paper establishes the theory of the inverse problem. Relying on practical examples, the reasoning demonstrates how the general source distribution formalism may be derived from a one-source formalism. The second section provides a numerical validation of the formalism whereas the third section describes an experimental one. The fourth section presents how the method could be extended for source detection, in order to obtain the localization of lumped sources on a large wiring system. Finally, the last section concludes with possible implications of the method in the future. They could be numerous in the experiment world, for the EM maintenance of bundles, for a better definition of bulk current injection (BCI) tests. In parallel, the method could also provide a new numerical strategy for using wire models in 3D codes.

2. From a discrete to a distributed source model

2.1. Recall of EM field-to-line coupling models

In the theory of field-to-line coupling on transmission lines, source terms are directly derived from the *incident* EM fields, that is to say, the field in the absence of wires. Two models, Taylor's and Agrawal's models ([8], [9]) are commonly used in the literature. A third one, developed by Rachidi [10], seems devoted to more specific power-line applications and, thus, will not be discussed in this paper.

In Taylor's model (figure 1), the coupling of an incident EM field on a transmission line is described by the application of a pair of per-unit-length current and voltage generators, "V_s" and "I_s". In the particular case of multiconductor lines, those generators are expressed in terns of vectors. The application of this model provides voltage and current everywhere on the line.

The voltage generator, V_s, comes from the derivative of the flux of the magnetic field, in an elementary cell.

$$V_s = j.\omega.h.H^o \qquad (1)$$

where "H^o" represents the transverse component of the magnetic field, and "h" the height of the line.

The current generator, I_s, comes from the derivative of the normal component of the incident electric field :

$$I_s = j.\omega.C.E^n \qquad (2)$$

where "C" represents the physical capacitance of the wire and "E^n", the normal component of the incident electric field. The transverse magnetic field and the normal electric field are supposed to be constant along the height of the line.

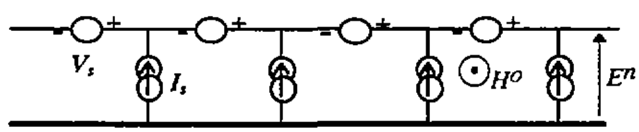

Fig. 1 : Taylor's field-to-transmission-line coupling model

The second model, Agrawal's model (figure 2), describes the field coupling with the application of distributed per-unit length voltage generators only, V_s, equal to the tangential component of the electric field "E_t".

$$V_s = E_t \qquad (3)$$

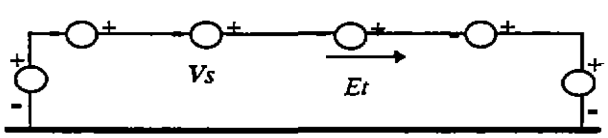

Fig. 2 : Agrawal's field-to-transmission-line coupling models

The important point to remember is that Agrawal's **model requires taking into account the electric field component at the extremities the line**. Everywhere on the line, the application of this model provides the actual current but only the "*scattered*" component of the voltage. The "*total voltage*" is obtained by simply adding the "*incident voltage*" component due to the incident normal electric field. Nevertheless, at the level of small size localized loads, the total voltage is approximated by the scattered voltage only.

From a theoretical point of view, those two methods are supposed to be valid in the thin wire approximation. For wires close to the reference or wires close to each other, additional terms, accounting for the deformation of the field have to be considered ([11], [12]). Nevertheless, recent application studies carried out by ONERA and Renault have demonstrated that Agrawal's model was sufficient when applied on complex topology cables inside complex structures ([4], [5]). In that case, the complexity of the structure naturally produces an averaging effect on the field distribution, which seems to make the correction field-terms non significant.

From a technical point of view, Agrawal's model is more convenient than Taylor's one. We will give here three main reasons :

1 - in Agrawal's model, only one kind of generator is required, whereas a voltage and a current generator are required in Taylor's model,
2 - in Taylor's model, the notion of height of a line in (1) is not always clearly defined in a complex geometry environment,
3 - in Taylor's model, the calculation of the "W_s" source wave, according to the general definition of the BLT equation [13], involves the summation of two terms related with each type of generators :

$$W_s = \int_0^L (V_s + Z_C \cdot I_s) \cdot e^{-(L-z)\gamma} dz \qquad (4)$$

where "γ" represents the propagation matrix of the line and "L", the length of the line.
The source wave can be interpreted as the "*collection*" at the end of the cable of all the distributed elementary source waves $(V_s + Z_C \cdot I_s)$ distributed along the cable, taking into account the phase shift due to their location. Two source waves must be considered for both propagation directions on the cable.
The contribution of voltage generator terms is easy to calculate. It is simply given by the integration of all the voltage generators along the line. On the contrary, the current generator counter-part requires first a multiplication by "Z_C", the characteristic impedance matrix of the tube. In Agrawal's model, this calculation does not exist.

Therefore, Agrawal's model is less time and memory consuming than Taylor's. In addition, it does not depend on the geometry of the line. Nevertheless, one has to be able to determine the tangential component of the electric field, which is generally much smaller compared to the main normal component in the vicinity of the reference structure. Practically, it is impossible to measure directly this component whereas a 3D code has enough precision to calculate it.

2.2. One-source inverse problem formalism

2.2.1. The theory

The proposed method is based on the use of Agrawal's model, chosen for the technical advantages previously mentioned. It consists in using a test-wiring, running at the same location as the actual cable, as a sensor of tangential electric field. The distributed currents along the test-wiring are the inputs of an inverse problem that provides the determination of those fields. Once the fields obtained, two kinds of applications may be considered :

1 - the fields may be introduced in any model of cable bundle running at the same location as the test-wiring. The user is then able to modify the model of the cable bundle without modifying the source terms,
2 - the constitution of data banks of distributed fields along different possible wiring paths, in order to optimize cable routings in the structure.

The fact of using the same generators for the test-wiring and the real wiring requires an important condition on the reference structure. This one must have good conductivity in such a way that no significant difference of potential can be observed under the lines. Indeed, this potential difference strongly depends on the value of the wiring. This condition is particularly important for low frequency problems.

The test-wiring must be chosen the most simple as possible to make the resolution of the inverse problem the most accurate. For cable modeling, precise models of one-wire transmission lines are available and easy to apply, which is not always the case for multiconductor models. Nevertheless, the test-wiring can be a network made of different single wire branches running in different places of the structure.

In addition, for practical applications in experiments, the measurements of currents on one-wire cables are straightforward and do not present the same technical drawbacks as the ones encountered on cable-bundles [14].

The one-source generator model deals with the case where the external excitation is described with only one voltage generator. To make the following demonstration easier, the test-wiring will be limited to only one wire branch, and will be called the "*test-wire*" (figure 3). In the "*real problem*", let us suppose that the test-wire is illuminated by the actual incident field. This produces a current " I^{real} " in one given position along the wire. The "*inverse problem*" deals with finding the voltage generator " V_s^{real} " which originated this current. The choice of the loads at both ends of the test-wire is not an important issue, but generally to obtain the highest value of I^{real}, the test-wire is chosen short-circuited at both ends.

The determination of V_s^{real} can be achieved as follows. In the "*elementary problem*", an elementary voltage generator " V_s^{el} " will create an elementary current" I^{el} " at the same location as I^{real}. If one is able to model the test-wire with a network formalism, I^{el} is straightforward to calculate. This is why test-wires or, more generally, test-wirings, have to be chosen the most simple as possible to avoid the requirement of heavy multiconductor models.

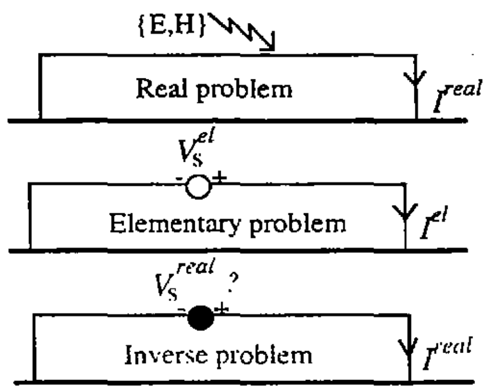

Fig. 3 : Different steps in the resolution of a single source test-wiring problem

Relying on the linearity of the problem, it is possible to state that the ratio of the two currents is equal to the ratio of the two generators that produce them. V_s^{real} is then directly derived :

$$V_s^{real} = \frac{I^{real}}{I^{el}} V_s^{el} \tag{5}$$

In (5), I^{el} is calculated and I^{real} is an input data of the real problem, that is to say, the test-wire inside the illuminated structure. Thus, this method is similar to the resolution of a simple inverse problem in which :

- the real response of the system is known,
- the model of the system is known,
- the source term producing the known response of the system is looked for.

2.2.2. Application

Whereas very simple, this type of transfer-function method can be really efficient. Especially, it provides precise rules to apply more general BCI tests. The example we have chosen comes from an experiment, held in 1993 on the EMPTAC (Electromagnetic Test-bed Aircraft), as a collaboration between ONERA, Centre d'Etudes de Gramat (CEG), FRANCE, and Phillips Laboratory (now Air Force Research Laboratory), Albuquerque, New-Mexico, on EM Topology [6].

One of the wiring problems analyzed during the experiment was to determine the coupling inside a well called the *"forward shielded volume"* (figure 4) when the aircraft was illuminated with an antenna called *"Ellipticus"* (figure 5). This antenna provides the same type of plane wave as *an "EMP DPH"* generator except that the signal is provided in frequency domain and the power is much lower. In the case of figure 4, it was reasonably assumed that most of the coupling on the wiring under study came from the coupling on the shielded wire running inside the cockpit. Indeed, the "forward shielded volume" had been specially designed to be hardened against EM interference. Therefore, the problem was to determine the equivalent voltage source term to apply on the cockpit shielded cable model.

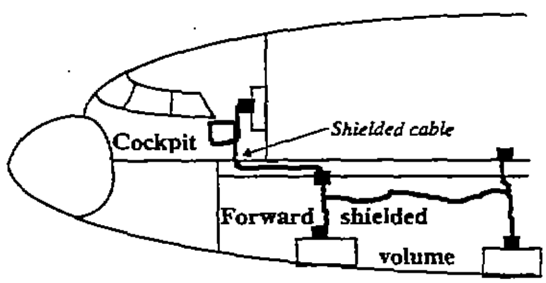

Fig. 4 : Wiring under study in the cockpit and forward shielded volume of the EMPTAC

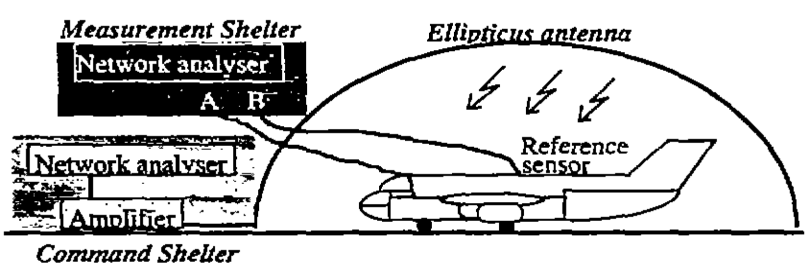

Fig 5 : Measurement principle on the EMPTAC aircraft under the Ellipticus antenna

So, at the time of the experiment, neglecting the internal cable coupling, it was decided to consider the shield of the cockpit cable as a test-wire short-circuited at both ends. The real current, I^{real}, due to the illumination was measured in one location of the cable and the elementary current. The elementary current, I^{el}, due an elementary voltage excitation at the same location was calculated with the CRIPTE code [15]. The real voltage generator V_s^{real} to apply on the real wiring was determined with (5).

Then, comes the whole interest of the method. The V_s^{real} voltage generator does not depend on the cable type, provided that the cable runs at the same location as the test-wiring. This way, V_s^{real} was applied to a full model of the real wiring problem, involving both external and internal domains. In other words, V_s^{real} has been applied identically on each wire of the equivalent model (shield and internal wires). Without modifying the source term, the CRIPTE code could calculate the response of the system in extreme grounding configurations. Two configurations of the shield connection to the structure were investigated :

- when the shield was perfectly connected to the structure at both extremities,
- when the shield was not connected to the structure at the level of the interface between the two volumes under study.

Figure 6 shows the voltages calculated between 300 kHz and 100 MHz in both configurations at the same test point inside the forward shielded volume. They are compared to direct measurements. Results are very good in low frequency (up to 10 MHz) where the resonance observed is due to the resonance of the airplane. At higher frequency, the resonance is a combination of the structure and the wiring resonance. Even if the average level is well predicted in both configurations, the accuracy is not as good as in low frequency. In fact, the limitation of the single generator problem appears clearly here. The accurate model does not require only one generator but a *distribution of several generators. Typically, the criterion to determine the number of generators is the same as* the one to define the size of elementary cells in 3D numerical models. If λ is the wave-length under study, the length on which a generator is applied on the test-wire should not be larger than $\lambda/10$.

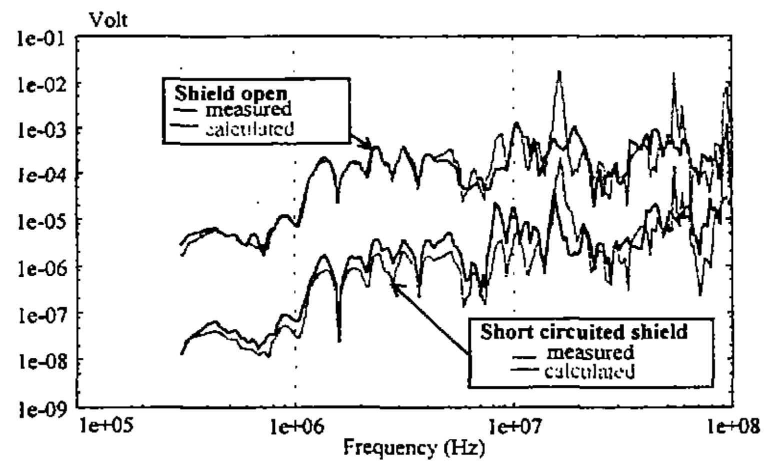

Fig. 6 : Response of the forward volume wiring in two configurations of the cockpit cable shield connection

The voltage generator Vs^{real} applied in the one-generator model is equivalent to the integral of all the generators distributed along the cable, without taking any phase shifting consideration. This is sufficient in low frequency because the phase shifting is not relevant because the current is uniform along the wire, and the transfer functions everywhere on the cable are the same. In high frequency, the average level is correctly predicted but the transfer functions obtained when measuring I^{real} at one extremity of the test-wire or the other are different and provide different results.

In this particular case where the test-wiring (the shield) is also the real wiring, it is important to notice that the restrictive condition on the good conductivity of the structure is not required anymore when the shield is short-circuited at both ends. Indeed, even if the difference of potential develops on the structure, under the shield, it remains the same in the test-wiring and real problem.

2.2.3. Generalization of the one-generator approach to distributed sources

In high frequency, the application of one generator describing the coupling on a tube is not sufficient. In 1995, the same kind of experiment as the one described in the previous section has been carried out on the EMPTAC at higher frequency, with the same Ellipticus antenna. The results presented now deal with the coupling inside the forward shielded volume between 100 MHz and 1 GHz. As previously, two extreme EM hardening configurations have been tested :

- when the door of the forward shielded volume was closed,
- when the door of the forward shielded volume was opened.

In a first step a metallic braid has been installed as a test-wire, short-circuited at each reinforcement bar inside the volume (figure 7-a). This way, the braid could be considered as a linear set of independent small test-wires. Currents have been measured between the bars and elementary one-generator inverse problems have been solved in both door aperture configurations. In a second step, the braid was replaced by a single one-wire cable (same length, same running path), but this cable was short-circuited at its extremities only (figure 7-b). The sources determined in both configurations have been distributed on the one tube topological model of this wire.

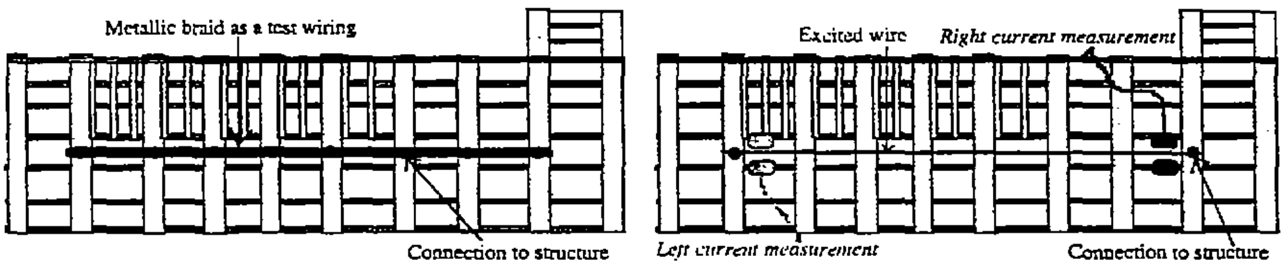

Fig 7-a : Test-wire configuration *Fig 7-b : Excited wire configuration*

Fig. 7 : Configurations of the test-wire and real wiring installed inside the EMPTAC forward shielded volume

Figure 8 displays the comparison of the calculated and measured currents in both configurations, at both extremities of the real wire. The two charts represent a current at one extremity of the wire. In order to get rid of the large number of resonance appearing in this frequency range, the data have been processed with a kind of energetic filter averaged in an adaptive bandwidth. The value displayed in figure 8 is equal to :

$$M = \sqrt{\frac{1}{f_2 - f_1} \cdot \int_{f_1}^{f_2} |S(f)|^2 . df} \qquad (6)$$

where :

- "S" is voltage or current signal at the test-point of interest (a current in this case),
- "f_2-f_1", the bandwidth, (" in this case 10 % of the frequency of interest, "f).

Both sets of curves reproduce correctly the coupling level at the ends of the wiring. Especially, one will notice that the responses are slightly different at the two ends of the cable. This result could not have been obtained without the distribution of several source terms.

Another additional comment can be issued from those curves. The transmission-line model seems to be perfectly able to predict correctly the coupling level, even at high frequency where the assumption of dominating TEM modes is usually considered as suspicious. Since this experiment, similar results have been obtained in [16]. Moreover, the energetic averaging of the data seems to provide a good way to visualize the coupling in highly resonating structures. A similar average, applied on the low frequency plots of the previous sections would have given a good agreement on the whole frequency range (figure 6).

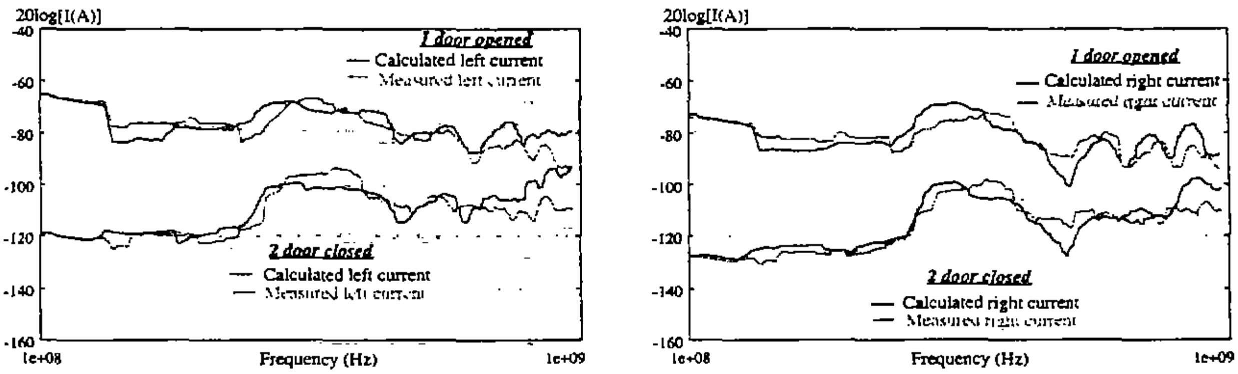

Fig. 8-a : Left extremity

Fig. 8-b : Right extremity

Fig. 8 : Current obtained at both extremities of the real wire inside the forward shielded volume

3. Distributed-source inverse-problem formalism

3.1. The theory

Short-circuiting a test-wire in different sections as depicted in section 2.2.3 removes all the convenience we were looking for in the research of the test-wiring methodology. Nevertheless, the example provides the basis of the demonstration of a multiple-source inverse-problem resolution of a multiple source inverse problem. The generalization of the method is directly inspired from the one dimension problem. Instead of one generator, the problem consists in determining "n" generators. To make the demonstration easier, an example with n=3 segments has been used (figure 9).

The real problem (figure 9-a):

The real problem is the one of the test-wire excited by an external field. This problem provides the three currents, "I_j^{real}", induced in each segment "j" of the test-wire. The sections are supposed short enough to consider the current constant on each of them. Typically, the length of a segment is chosen in "λ/10", where "λ" is the smallest wavelength of the problem.

The elementary problem (figure 9-b):

The elementary problem can be considered as the superimposition of three elementary problems. Each elementary problem is made by the excitation of one segment with a serial voltage generator, "V_i^{el}". For each elementary problem, the application of V_i^{el} produces an induced current "$I_j^{el}(i)$" in each of the j^{th} segments. Applying the superimposition theorem, the total current, "I_j^{el}", flowing in a segment "j" is equal to the sum of the elementary currents in each elementary problem. Therefore :

$$I_j^{el} = I_j^{el}(1) + I_j^{el}(2) + I_j^{el}(3) \qquad (7)$$

Applying the linearity principle, each elementary current $I_j^{el}(i)$ is related with a linear transfer coefficient, "f_{ji}", to the elementary source $V_s^{el}(i)$ that gave birth to it. In the case of our three-segment test-wire, the following linear relations can then be written :

$$\begin{aligned} I_1^{el} &= f_{11} \cdot V_s^{el}(1) + f_{12} \cdot V_s^{el}(2) + f_{13} \cdot V_s^{el}(3) \\ I_2^{el} &= f_{21} \cdot V_s^{el}(1) + f_{22} \cdot V_s^{el}(2) + f_{23} \cdot V_s^{el}(3) \\ I_3^{el} &= f_{31} \cdot V_s^{el}(1) + f_{32} \cdot V_s^{el}(2) + f_{33} \cdot V_s^{el}(3) \end{aligned} \qquad (8)$$

Relation (8) can be generalized in the simple matrix form as :

$$\left[I^{el}\right] = [f]\left[V_s^{el}\right] \qquad (9)$$

where in our case ;

$$\left[I^{el}\right] = \begin{bmatrix} I_1^{el} \\ I_2^{el} \\ I_3^{el} \end{bmatrix} \quad ; \quad \left[V_s^{el}\right] = \begin{bmatrix} V_s^{el}(1) \\ V_s^{el}(2) \\ V_s^{el}(3) \end{bmatrix} \quad \text{and} \quad [f] = \begin{bmatrix} f_{11} & f_{12} & f_{13} \\ f_{21} & f_{22} & f_{23} \\ f_{31} & f_{32} & f_{33} \end{bmatrix} \qquad (10)$$

Hereafter, "f" will be called the "*Green's function matrix*" of the test-wiring. Indeed, its definition is very similar to a Green's function relating the response of a discrete system a series of to discrete excitations. It can be also noticed that if each elementary voltage excitation $V_s^{el}(i)$ is chosen equal to 1 volt, each coefficient f_{ji} is directly equal to $I_j^{el}(i)$.

The inverse problem (figure 9c) :

Therefore, the inverse problem deals with finding, in each segment "i", the actual voltage generators, "$V_s^{real}(i)$" giving birth to I_j^{real}, the currents in each segment "j" of the real problem. Because of the linearity of the problem, the following relation can be written :

$$\left[I^{real}\right] = \left[f\right]\left[V_s^{real}\right] \tag{9}$$

where in our case :

$$\left[I^{real}\right] = \begin{bmatrix} I_1^{real} \\ I_2^{real} \\ I_3^{real} \end{bmatrix} \quad \text{and} \quad \left[V_s^{real}\right] = \begin{bmatrix} V_s^{real}(1) \\ V_s^{real}(2) \\ V_s^{real}(3) \end{bmatrix}$$

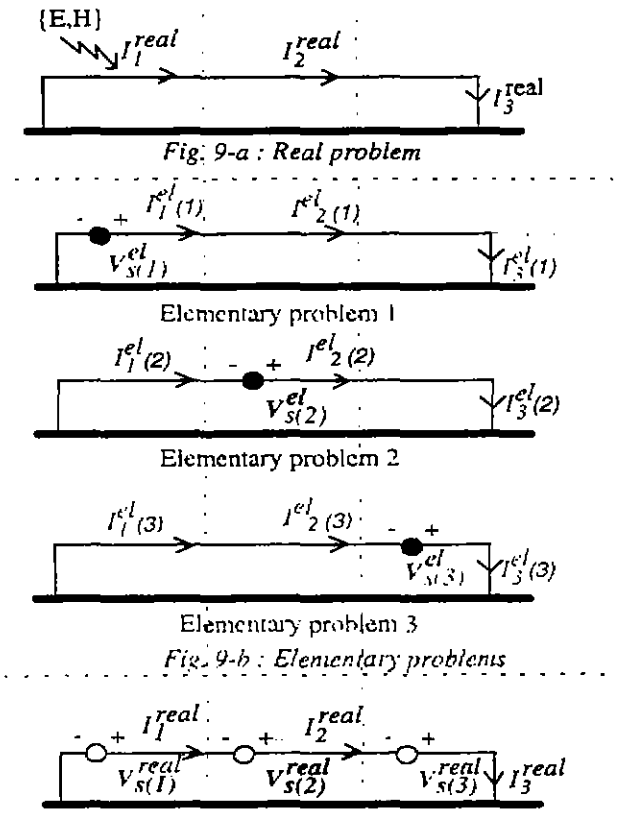

Fig. 9-a : Real problem

Fig. 9-b : Elementary problems

Fig 9-c : Inverse problem

Fig. 9 : Different steps in the resolution of a three segment test-wire problems

By choosing the elementary voltage generators equal to 1 volt, "f" is directly obtained from (8). Then, from (9), the distribution of the real voltage generators is obtained by simple inversion of "f".

$$\left[V_s^{real}\right] = [f]^{-1} \cdot \left[I^{real}\right] \qquad (10)$$

3.2. Practical application procedure

The way to apply this method in practical experimental problems can be defined through the following rules :

- step 1 - remove the excited cable and install the test-wire at the same location,
- step 2 - measure currents in different points of the test-wire (the location of the test-points is conditioned by the higher frequency under study).
- step 3 - numerically determine the Green's function matrix of the test-wire,
  - 3-1 : model the test-wiring with a transmission-line network model,
  - 3-2 : calculate the current in the different test-points for all the segment excitations with a 1 Volt generator,
- step 4 - calculate the generators of the real problem from (10),
- step 5 - apply the real sources on the topological model of the real cable.

In addition, one must keep in mind that the condition on the good conductivity of the reference, already mentioned in 2.2.1, is also required.

3.3. Numerical validation

The first validation proposed is entirely numerical. The calculation of the reference problem and the real test-wiring problem are supplied with a 3D code. The computer code used is the Method of Moment (MoM) code "*CADENCE*" developed at ONERA. Figure 10 gives the geometry of the problem. A wire is laying on an infinite metallic plane and is running in two directions (path1 and path 2). The length of path 1 is 1 m, decomposed in two parts. On the first 50 cm, the cable has a 10 cm height whereas, on the remaining 50 cm, it has a 5 cm height. Path 2 is 1.65 m long with a constant height equal to 5 cm. The wire is loaded by a load R_0 at the extremity of path 1 and by a load R_1 at the extremity of path 2. The excitation is provided by a 50 cm monopole antenna driven by a 1 Volt generator at its base.

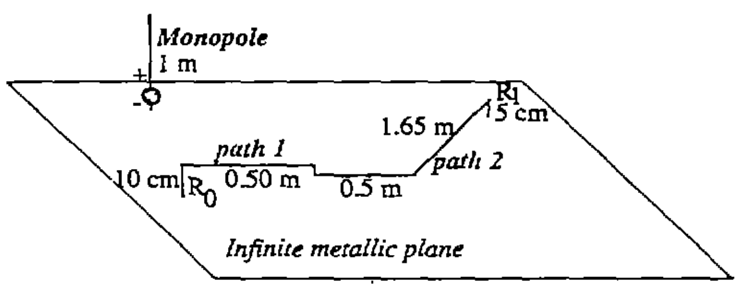

Fig.10 : Geometry of the numerical problem

The reference plane being infinite, the 3D meshing has been simplified by taking into account the wire and the monopole electrical image with respect with the metallic plane (figure 11). The 3D modeling has been used for two purposes :

1 - to determine the distribution of real currents along the test-wiring. The location of the test-points has been made in such a way that a λ/5 criterion has been respected. In this case, R_0 and R_1 are equal to short-circuits,

2 - to determine the load voltage response of the real wiring for different load configurations. In this case, to demonstrate that the cable can be different of the test-wire, the radius of the real cable has been chosen greater than the test-wire one.

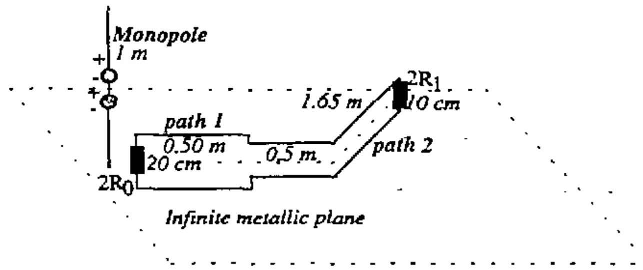

Fig. 11 : Principle of the modeling applied in the MoM numerical code

The determination of the test-wire Green's function has been achieved with the CRIPTE code [15]. In the modeling, the segments are described by several tubes. The tube length is determined as respect with a λ/5 criterion. Nevertheless, tubes are introduced each time the characteristic of the line changes (height, direction), even if the length of the tube is inferior to the criterion. This is particularly the case for the modeling of the vertical parts of the line. They are modeled as transmission lines whose characteristics are the same as the horizontal line connected to them [17]. The Green's function matrix is obtained by calculating different source configurations where each tube is excited with a voltage generator and the resulting current is calculated on all other tubes.

Let us precise that, at the time of the calculations described in this paper, the capability to determine current and voltage everywhere on a tube was not already implemented in the CRIPTE code [18]. This is why the splitting of a test-wire in several elementary tubes was required, even if the per-unit length characteristics of those tubes were identical. Nowadays, the method could take advantage of this new capability of the code to reduced calculation time and memory.

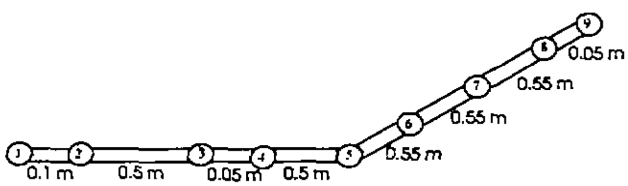

Fig. 12 : Topological model of the test-wire for the Green's function matrix determination

Combining the Green's function matrix with the real currents computed with the 3D code, the real voltage generators can be determined and used in the CRIPTE code for other configurations, keeping on using the same source terms. Figure 13 gives an example of application that can be carried out. It represents the cable network of the real cable on which junctions 5 and 6 can be easily modified to account for different terminal loads.

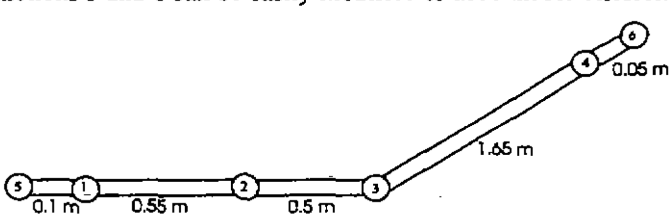

Fig. 13 : Topological network used for the determination of the response of the real wiring

As an example, figure 14 presents the voltage obtained on junction 5 and junction 6 when R_0= 1 Ω and R1 = 50 Ω. *Figure 15 presents the same result when* $R_0 = R_1 = 1$ Ω. *In both cases, up to 100 MHz , the voltage* obtained is very close to the actual response determined with the 3D code. Those results fully demonstrate the accuracy of the method. *In high frequency (from 50 MHz) there may be some slight difference between the plots,* due to the fact that the λ/5 criterion is not sufficient. The difference may also come from the fact that the transmission-line model does not account for the non TEM fields existing at the discontinuities. Particularly, the fact of modeling the vertical extremities with transmission line can be a great approximation when the value of the load increases. *In addition, the loads are not localized in the 3D code whereas they are infinitely small in the* network code.

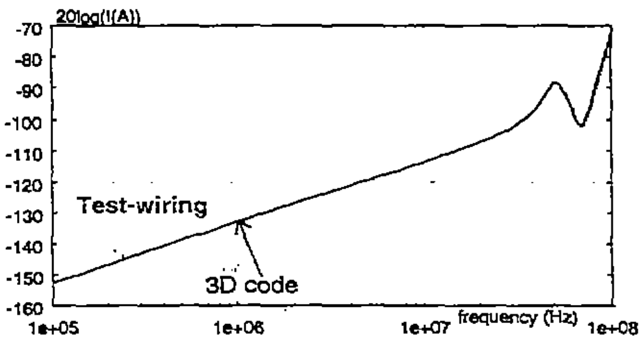

Fig.14-a : Junction 5

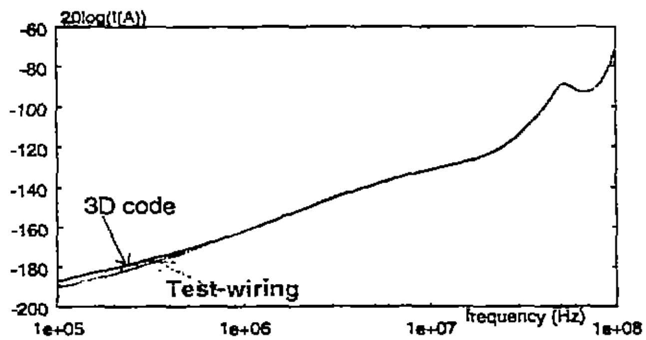

Fig.14-b : Junction 4

Fig. 14 : Response of the actual wiring for R0 = 1 Ω and R1 = 50 Ω

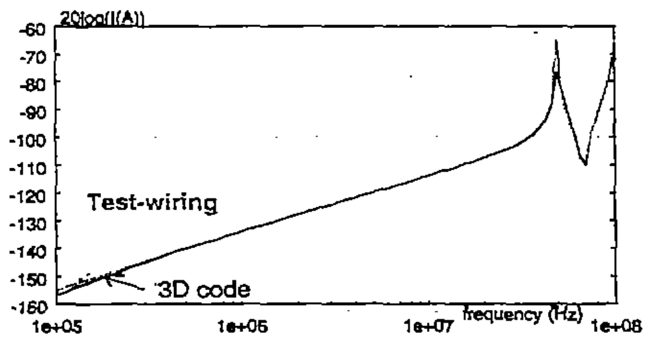

Fig. 15.a : Junction 5

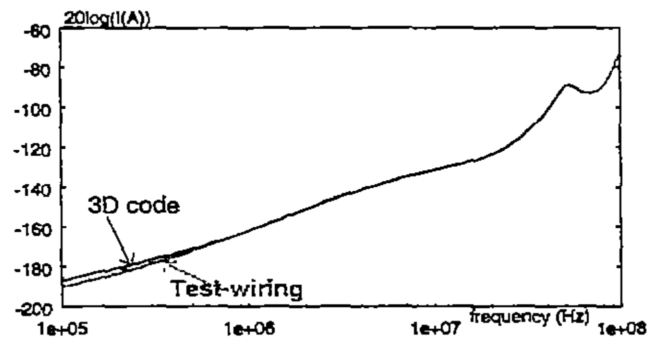

Fig.15-b : Junction 4

Fig. 15 : Response of the actual wiring for R0 = 1 Ω and R1 = 1 Ω

As a complement to the signal determination on the line, it can be interesting to analyze how the generator distribution calculated from the test-wire method may match the incident tangential field on the wiring path. Figure 16 presents two mappings of the voltage generators (figure 16-a) and the tangential electric field (figure 16-b) as a function of the position and the frequency. The two surfaces present the same levels and the same variations. Particularly, the generator surface reproduces correctly the breakdowns of the field occurring at the vertical positions of the line (at the level of the ends and at the level of junction 2). At those positions, the magnitude is slightly different due to the great approximation of the vertical parts as transmission lines. Nevertheless, the overestimated values are compensated around an average value. In fact, because of the integral formulation of the source waves in the line equations (see relation 4), no significant discrepancy is observed in the response of the line.

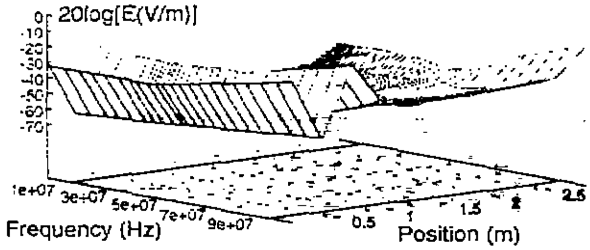

Fig.16-a : Generators deduced from the test-wire method

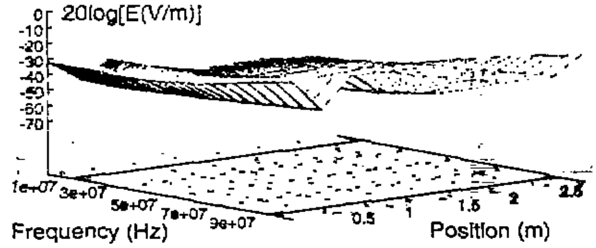

Fig.16-b : Tangential electric fields

Fig. 16 : Mapping of the generators and tangential fields along path 1 and path 2

3.4. Experimental validation

The experimental validation presented here has been carried out as a part of an experiment on the body car of a RENAULT Laguna car (a metallic structure) ([4], [5]). During the experiment, a linear test-wire has been substituted to one particular path of the prototype wiring installed inside the body car. The car being excited by a quasi-plane wave provided in time domain by a semi-rhombic antenna (SSR, from Centre d'Etudes de Gramat, France), currents have been measured along the test-wire on positions respecting a $\lambda/5$ criterion.

The Green's function matrix of the test-wire has been determined with the CRIPTE code by meshing the test-wire with elementary tubes. Then, a real four-wire cable of the prototype wiring has been reinstalled in place of the test-wiring (figure 17-a). Reference measurements have also been achieved for different load configurations at the end of the four-wire cable (figure 17-b). Two kinds of measurements were carried-out :

- voltage at port 1 (always loaded to 50 Ω) because of the input impedance of the digitizers,
- bulk current measurement at the level of end B.

On the other hand, numerical simulations have been carried out on with the CRIPTE code on the model of the four wire-cable, applying the source terms coming from the test-wiring method.

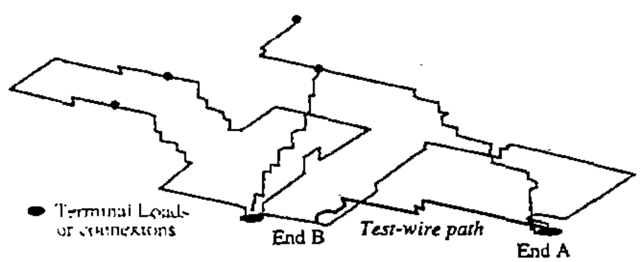

Fig 17-a : Location of the wiring path among the whole prototype wiring

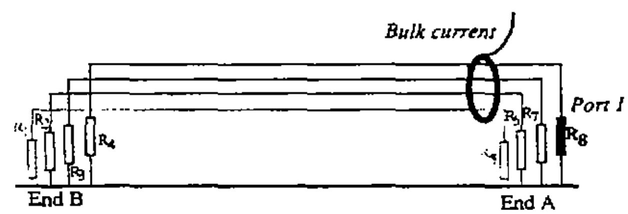

Fig 17-b : Terminal loads and location of the voltage an current measurements

Fig.17 : Wiring path under study in the Laguna body car

Figure 18-a to 18-d presents the results obtained with the test-wiring method in two load configurations, A and B, displayed in table 1. The calculation plots are superimposed with the reference measurement carried out directly on the cable. All the measurements have been achieved in time domain, whereas the CRIPTE calculations have been performed directly in frequency. Hence, the Fourier processing to convert measurements in frequency domain may contain errors in very low frequency because of the lack of memory of the digitizers. Nevertheless, the agreement between the superimposed plots is obvious. Especially, in high frequency, the

resonance seems to be correctly predicted up to 200 MHz. Overvalues predicted by the calculation could be widely improved with a more accurate modeling of the test-wiring and the four-wire cable network, especially by accounting for the frequency dependence of its per-unit-length parameters.

Impedance	Configuration A	Configuration B
R_1	Open circuit	Open circuit
R_2	0 Ω	Open circuit
R_3	0 Ω	0 Ω
R_4	0 Ω	0 Ω
R_5	50 Ω	50 Ω
R_6	Open circuit	0 Ω
R_7	Open circuit	0 Ω
R_8	50 Ω	50 Ω

Table 1 : Terminal loads in configurations A and B

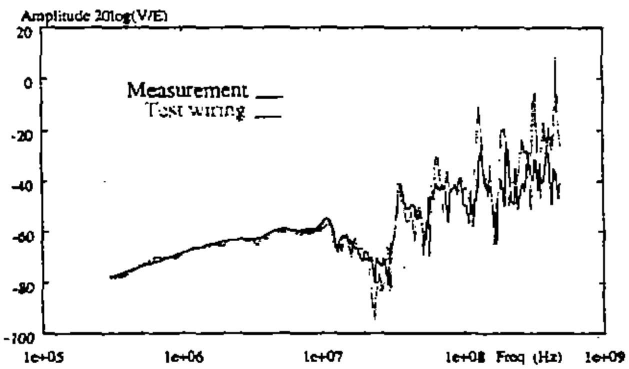

Fig 18-a : Bulk current in configuration A

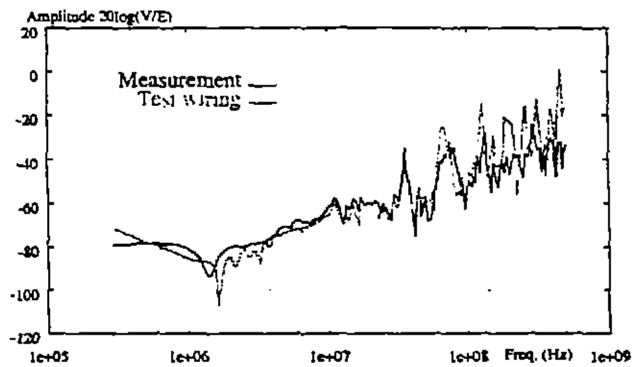

Fig 18-b : Voltage on port 1 in configuration A

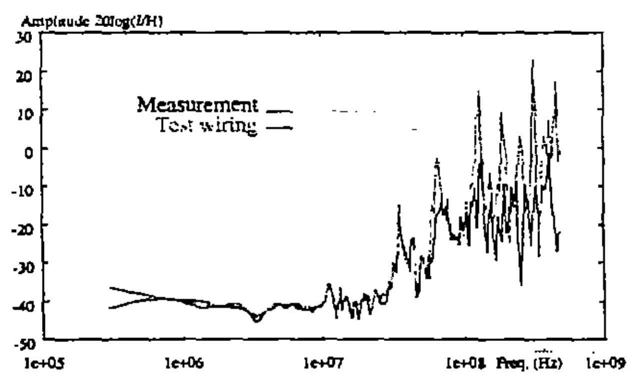

Fig 18-c : Bulk current in configuration B

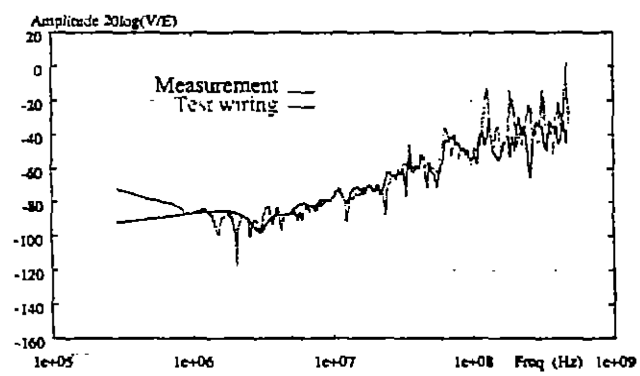

Fig 18-d : Voltage port 1 in configuration B

Fig 18 : Modeling results obtained with the test-wiring method and comparison with direct measurements

4. Using the test-wiring method for a source detection

As depicted on figure 16, the test-wiring method is also a good method to obtain a good idea of the tangential electric field distribution along a wiring path. In this present section, we would like to show that the application could go farther, in terms of a detection of a localized source existing on a large cable system.

To demonstrate this capability, we have performed the canonical experiment presented in figure 19. A transmission line, 1.3 m long, is installed on metallic plane reference. This long wire is considered as a test-wire. Between 0.3 cm and 0.6 cm a small wire is located in parallel to the long wire short-circuited at both ends. A current injector is applied on the small wire and induces a voltage interference on the long wire.

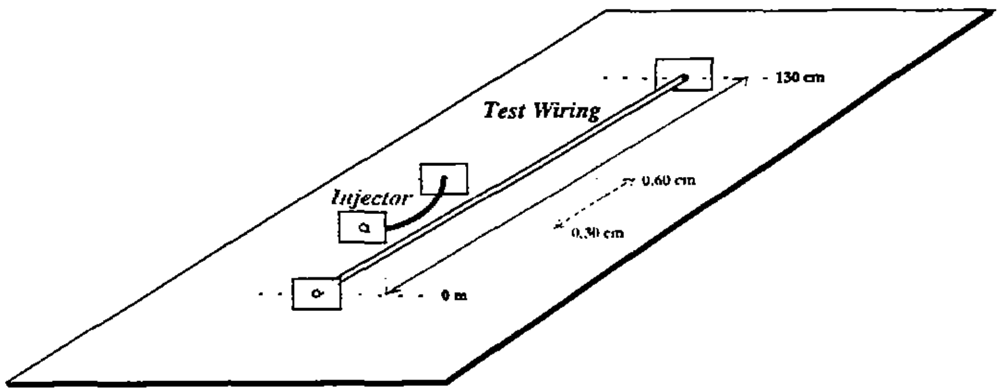

Fig. 19 : Experimental set-up for the determination of the injector position with the test-wiring method

This problem is a detection problem. Determining the current all along the test-wire and, then, determining the distribution of equivalent voltage generators, is it possible to figure out the location of the injection wire? Two approaches have been achieved : one numerical, one experimental. Because of the simplicity of the problem, involving only cable-coupling phenomenon, the numerical problem has been entirely treated with the CRIPTE code. The experimental problem has been solved classically by directly measuring the current distribution along the test-wire.

It must be mentioned that, in the modeling of the wire, the vicinity of the injector had to be taken into account with a 30 cm tube. Indeed, the small wire is a part of the structure and so, modifies the per unit length of the test-wire.

Figure 20 and 21 present on a flat surface the voltage distribution obtained as a function of the frequency and the position along the wire. In high frequency, the result obtained with the numerical problem is perfect and provides clearly the localization of the source between 0.3 and 0.6 cm. In low frequency, up to 5 MHz the results present errors that will be attributed to numerical precision.

The result obtained with the experimental results is less obvious. As for the previous results, the errors will be attributed to the lack of precision of the input data. In low frequency (up to 10 MHz), the result is equivalent to a source distributed on the whole wire. Even if the location of the source is not predicted, this result would predict correctly the real response of a wiring, because the phase is not important in low frequency.

In the medium frequency range, between 20 MHz and 100 MHz, the excitation zone is well predicted. In high frequency, errors appear at the level of resonance where the precision of the measurements is certainly not sufficient. Nevertheless, between two resonance peaks, the excitation zone is correctly predicted.

One will notice that the magnitude scales in the numerical and experimental problems are not the same. This is because in the numerical problem the frontiers of the excitation zone are very well defined and provide a real step in the source distribution. On the contrary, in the experimental problem, the borders are not as precise because of an averaging effect occurring at their level. This makes the total source being distributed slightly outside the excitation zone.

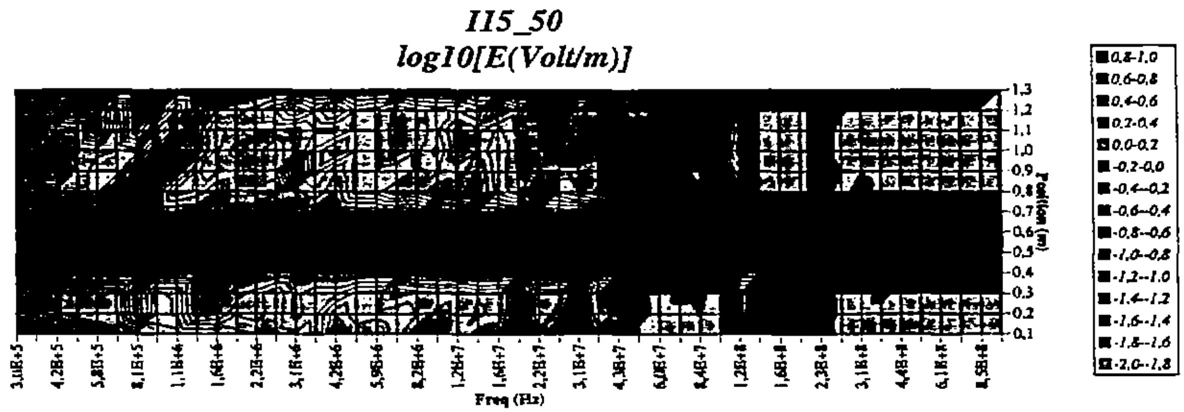

Fig. 19 : Voltage generator distribution obtained from the numerical simulation, as a function of frequency and position along the test-wire

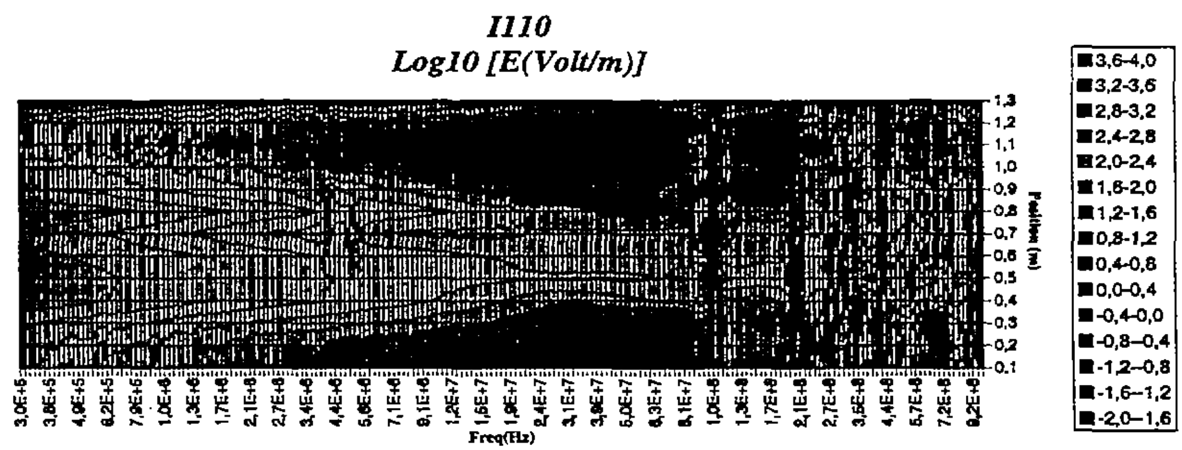

Fig. 20 : Voltage generator distribution obtained from measurements, as a function of frequency and position along the test-wire

5. Conclusion : perspectives of the method

The objective of this paper was to demonstrate a convenient technique to determine the voltage source terms to apply on cable-network transmission-line models of wiring excited by external EM fields. Assuming linearity, the method is based on the resolution of a simple inverse problem. The inputs of the problem are the following :

- the current response of a test-wiring, installed at the same place as the actual wiring. Those distributed currents can be measured easily if the test-wiring branches are made of one-wire cables,
- the Green's function matrix of the test-wire, entirely computed with a network transmission-line model. This matrix is obtained by exciting, one after the other, different sections of the transmission-line network model of the test-wiring and by collecting the distributed induced currents.

The first typical application is for cable-coupling prediction. Provided that the structure has a good conductivity, the generators do not depend on the type of wiring having been used to determine them. Consequently, in a numerical approach, the sources can be used for different cable models running at the same location as the test-wire. This way, the influence of the number of component wires and the terminal connections can be easily and quickly investigated using always the same source terms.

The second typical kind of application, closely related to the first one, is for estimating the field threshold on a possible wiring path. Indeed, the generators are directly related to the incident tangential fields on the wiring.

Finally, a third kind of application is for the detection of localized sources. The technique still needs some improvements. Nevertheless, it provides promising results for future investigations (for slit leakage for example).

Therefore, the test-wiring method is mainly devoted to experiments on complex structures. Even based on physical approximations, the results obtained on complex structures are really satisfactory. From a theoretical point of view, the installation of the test-wiring requires to remove the wiring under study. It could be interesting to analyze the sensitivity of the method when the actual wiring is not removed when the test-wiring is installed. If the difference is low compared to the rigorous method, the modified technique could be used for the EM maintenance of bundles, within a special wiring could be devoted to a test-wiring function. Even if such a consideration seems really realistic, further investigations have to be carried out in this domain.

In addition, the test-wiring could provide a new way of applying the BCI method, commonly used in industrial world. Most of the time, the method is falsely understood as the injection of the current that has been measured under illumination whereas the voltage generator originating this current should be injected. Secondly, the use of multiple injectors would widely improve the results obtained on a large scale system as it has been demonstrated for the measurement of scattering parameters with a set of current probes [19].

Although mainly oriented to experiments, this approach does not exclude applications in 3D codes. On the contrary, one could think that it legitimates the constant will of people involved in 3D numerical techniques to introduce thin wires in their models. Indeed, the thin wires are supposed to represent cable bundles but do not account for the great complexity of the physics of coupling inside a bundle (wire to wire coupling, attenuation due to non uniformity). However, those thin wires could easily be considered as test-wires, allowing one to derive the tangential field distribution. Then, the response of the actual wiring could be easily calculated with a cable-network-code.

References

[1] C. E. Baum : The Theory of the Electromagnetic Interference Control. Interaction Notes. Note 478, December 1989 and, *Modern Radio Science 1990*, pp. 87-101, Oxford University Press.

[2] CRIPTE code users guide, ESI/ONERA, 1997

[3] J. P. Parmantier, P. Degauque : Topology Based Modeling of Very Large Systems. *Modern radio Science 1996*. Edited by J. Hamelin. Oxford University Press. pp. 151-177.

[4] L. Paletta, P. Dumas, J. P. Parmantier : Utilisation du champ électromagnétique tangentiel comme terme source dans les problèmes de Topologie Electromagnétique, Proceedings of the French CEM meeting, Lille, 3-5 September 1996, pp. 241-248. (in French).

[5] I. Paletta, P. Dumas, J.P. Parmantier, J.C. Alliot : EMC prediction based on the combined use of a three dimension and a cable-network approach. IEEE Trans. on EMC (submitted in 1998)

[6] J. P. Parmantier, V. Gobin, F. Issac, I. Junqua, Y. Daudy, J.M. Lagarde : An Application of the Electromagnetic Topology Theory on the Test-bed Aircraft, EMPTAC, Interaction Notes, Note 506, November 1993.

[7] J. P. Parmantier, V. Gobin, F. Issac, I. Junqua, Y. Daudy, J.M. Lagarde, L. Paletta : ETE III : Application of Electromagnetic Topology on EMPTAC, Interaction Notes, Note 527, May 1997.

[8] C.D. Taylor, R.S. Satterwhite et C.W. Harisson : "The Response of a Terminated two-wire Transmission Line Excited by a Nonuniform Electromagnetic Field", IEEE Trans. on AP, Vol. 13, N° 6, November 1986, pp. 987-989.

[9] A.K. Agrawal, H.J. Price, S.H. Gurbaxani : "Transient Response of Multiconductor Transmission Lines Excited by a Nonuniform Electromagnetic Field", IEEE Trans. on EMC, Vol. 22, N° 2, May 1980, pp. 119-129.

[10] F. Rachidi : Formulation of Field to Transmission Line Coupling Equations in Terms of Magnetic Excitation Field, IEEE Trans. on EMC, Vol. 35, N° 3, August 1993.

[11]K.S.H Lee : Two Parallel Terminated Conductors in External Fields, IEEE Trans. on EMC, Vol. 20, N° 2, May 1978, pp. 288-296.

[12] B. L. Michielsen : Accounting for Dielectrics in EM field to cable coupling. IEEE Trans. on EMC (submitted in 1998).

[13] C. E. Baum, T. K. Liu, F. M. Tesche : On the Analysis of General Multiconductor Transmission-Line Networks, Interaction Notes, Note 350, November 1978; also in C.E. Baum, Electromagnetic Topology for the Analysis and Design of Complex Electromagnetic Systems, pp. 467-547 in JE. Thomson and H. Leussen (eds.), *Fast Electrical and Optical measurements*, Vol. 1, Martinus Nijoff, Dordrecht, 1986.

[14] R. L. Gardner, J. L. Gilbert, L. Baker : Analytic treatment of cable bundles with large numbers of component wires. Interaction Notes. Note 450. February 1983.

[15] CRIPTE code users guide, ESI/ONERA, 1997.

[16] F. Issac, F. Hoeppe, P. Levesque, F. Boulay : Analyse de mécanismes de couplages sur une structure multicavités. Proceedings of the 9th conference on EMC. Brest, 8-12 June 1998, pp. B4-20,B4.25.

[17]E.F. Vance : Coupling to Shielded Cables, Krieger Publishing, 1987.

[18]J.-P. Parmantier, B. Michielsen, S. Bertuol, X. Ferrières : Améliorations dans le logiciel CRIPTE : code LAPLACE, création de tubes, calculs en des positions intermédiaires sur un tube, RTS ONERA n°12/6767 PY, February 1997 (in French).

[19] J. P. Parmantier : Méthodes pour le traitement du couplage électromagnétique sur le câblage d'un système de grande dimension, ONERA's report, RTS 12/6727 PY, February 1996. (In French).